JOURNAL OF MATERIALS SCIENCE 32 (1997) 6029–6038

TiN thin films deposited by filtered arc-evaporation: structure, properties and applications

I. KONYASHIN*
Hard and Refractory Metals Research Institute, Warshavskoye Highway 56, Moscow, 113638 Russia

G. FOX-RABINOVICH
RIMET Co., P.O. Box 167, Moscow, 125239 Russia

A. DODONOV
VIT Ltd, Uritskogo 40-58, Istra, Moscow Reg., 125675 Russia

A brief description of a plasma-optic system intended for filtered arc-deposition and the influence of its operational parameters on the deposition rate of TiN thin films are presented. A comparison of the microstructure, hardness, toughness, crystal lattice parameter, residual stresses, adhesion, performance and some other properties of TiN coatings deposited using either filtered arc-evaporation or conventional steered arc-evaporation techniques are given. The TiN coatings obtained by filtered arc-deposition are found to have a nanometre-grained structure, be highly uniform, smooth and droplet-phase-free. This leads to obtaining higher values of their hardness, toughness and adhesion compared with conventionally deposited TiN coatings, which results in improved performance of these coatings in wear and sliding applications.

1. Introduction

At present, thin TiN films deposited by use of arc-evaporation physical vapour deposition (PVD) are employed in industry as wear- and corrosion-resistant coatings on a large scale. There are some problems in the conventional arc-evaporation PVD technique, which lead to deterioration of the properties and structures of the conventionally deposited films.

One problem is related to the presence of macroparticles composed of the cathode material in the coating volume (the so-called "droplet phase") [1–3]. These macroparticles are ejected from the cathode source and can reach several tens of micrometres in size. The droplet phase when present in the coating volume leads to degradation in the coating hardness, surface roughness and performance properties. The presence of this phase at the substrate–coating interface can result in relatively poor adhesion of the coating. In applications where excellent surface roughness of the coating is essential, poor coating roughness caused by the presence of the droplet phase makes the coating inoperative.

The employment of steered arc-evaporation PVD allows the amount of the droplet phase to be noticeably reduced [4–7]; however, complete elimination of macroparticles in the coating is not feasible in this way.

There is also a problem concerning the procedure of heating the substrate up to deposition temperatures prior to coating. Typically, this procedure is performed by use of high-energy ions of refractory metals evaporated from the cathode. Unfavourable interaction of these ions with either hard-metal or steel substrates was determined to lead to substrate decarburization as a result of formation of a thin TiC layer due to carbon diffusion from the substrate [8–11]. The TiC thin layer, initially formed on the substrate surface as a result of this interaction, was determined to be comprised of a lot of pores and structural defects, which appeared to result in a decrease of the coating adhesion and other mechanical properties [11].

Problems related to the possibility of regulation of average grain size and crystal shape of thin coatings deposited by conventional arc-evaporation techniques also take place. Typically, these coatings have relatively coarse columnar structure [12], which results in their relatively poor resistance to cracks propagating from the surface towards the substrate–coating

* Corresponding author. *Present address*: Max Planck Institute for Metals Research, Heisenbergstr. 5, Stuttgart D-70569, Germany.

0022–2461

interface. In most cases, it is difficult or impossible to obtain fine- or nanometre-grained microstructure of the coatings by varying deposition parameters of the conventional arc-evaporation PVD.

One way suitable for eliminating the problems mentioned above was shown to be control of the evaporation path by magnetic or electrostatic fields and regulation of the energetics of the deposition process by use of a substrate bias voltage. The employment of magnetic or electrostatic fields for the control of the evaporation path allows the complete elimination of macroparticles in the coating volume to be achieved. Uncharged macroparticles present in the plasma are not affected by the fields and can be filtered off. A quarter segment of a torus is usually utilized to cause the plasma to flow as a curved path leaving the macroparticles to collide onto the inside of the filter. The basic principles of filtered arc-evaporation and some properties of the hard coatings deposited in this way have been reported in [13–28].

Smooth, hard films of TiN and other nitrides were deposited by reactive filtered arc-evaporation and some properties of these films were studied in [24]. A range of thin films were deposited using Si, Ti, Sn, etc., cathodes with the aid of filtered arc-evaporation in [15–28].

Meanwhile, though some properties of hard coatings deposited by filtered arc evaporation have been studied before, their structure and characteristics appear to be strongly affected by the method of filtering, design of the filtering arc-evaporation system and the deposition parameters employed. Moreover, there is almost no information in the literature about structure and properties of these coatings in comparison with coatings of the same composition obtained by conventional PVD techniques under similar deposition parameters. Furthermore, many important properties (e.g. fracture toughness) of such coatings have not yet been investigated. There is no information in the literature on the performance of these coatings as compared with those of the conventionally deposited ones in sliding and in cutting tool applications. The aim of this study is to investigate the influence of filtering plasma streams in the magnetic field on the deposition rate, structure, some properties and performance of thin TiN films in comparison with those obtained by use of conventional steered arc-evaporation PVD.

2. Experimental procedure

Hard-metal of M20 grade and high speed steel (HSS) of R6M5 grade were employed as substrates in the present study. The inserts were ground and sand blasted to obtain a surface roughness of around 0.63 μm and then ultrasonically cleaned in alcohol before the deposition procedure. Preliminary polishing of the steel specimens to a roughness of 0.08–0.16 μm was performed prior to examining the fracture toughness, microhardness and adhesion of the films.

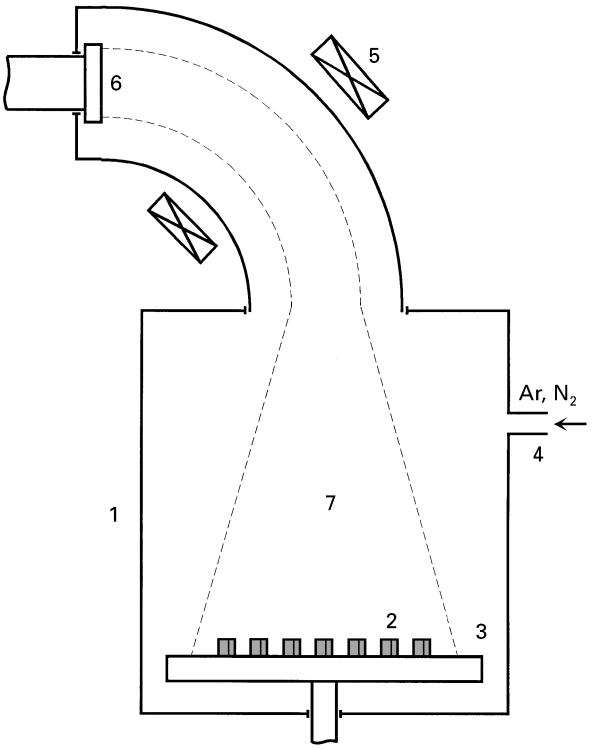

Figure 1 Schematic drawing of the filtered arc-evaporation system: (1) the PVD unit body, (2) substrate, (3) substrate holder, (4) feeder of gases, (5) body of the filtered arc-evaporation system together with an induction coil, (6) cathode, and (7) plasma path.

The coatings were deposited employing a standard unit of steered arc-evaporation PVD of NNV-6.6-I1 type with and without the use of the filtered arc-evaporation system (FAES)*, which is described below. FAES is removable and used to equip conventional units of arc-evaporation PVD. All the deposition processes were carried out at a substrate temperature of around 700 °C for the cemented carbide substrate and 500 °C for the HSS one; the temperatures were measured by an optical pyrometer. Heating the substrate up to the deposition temperature was performed by Ti ions in the case of the conventional PVD procedure and by Ar ions when applying filtered arc-deposition at the substrate biasing value of 1 kV. After obtaining the required substrate temperature, the substrate biasing value was reduced and nitrogen fed to deposit TiN films.

FAES was utlilized in the present study to deposit TiN films. The system was shown to affect the physicochemistry of plasmochemical processes significantly when depositing refractory compounds due to an increase in the ionization rates of both metals and reactive gases [24, 27]. The system included a hollow steel tube about 300 mm in diameter, which was a quarter segment of a torus (Fig. 1). The tube was installed on the body of a standard unit of the arc-evaporation PVD instead of on a conventional arc-evaporator. An induction coil, which created a magnetic field needed to control the plasma path, was placed inside the tube. The induction coil, tube

* FAES has been designed and is manufactured on a large scale by VIT Ltd, Moscow Region, the Russian Federation.

body, body of the PVD unit and cathode were electrically isolated from each other. There was a special device for controlling electric and magnetic parameters of the FAES.

Regulation of the plasma flow in the FAES is based on the principles of plasma-optics. The influence of the magnetic field upon the plasma flow allows the radial electric field to appear; as a result, regulation of the plasma path inside the internal volume of the FAES can be achieved in this way. Whereas only electrically charged particles are focused in the FAES, uncharged particles are not affected by the magnetic and electric fields. The uncharged particles when flying from the cathode surface parallel to the cathode axis do not reach the substrate surface and are deposited onto the inside of the tube, but ions are bent and focused on the substrate surface. The value of the continuous current running through the magnetic coil affects the distribution of the ion flow density. The body of the FAES is biased with regard to the PVD unit body, because employment of the substrate biasing is not enough to achieve a suitable value for the deposition rate. The FAES allows the substrate to be heated up to the deposition temperature by use of Ar ions, which is hardly achievable when applying a conventional arc-evaporation PVD unit. This was shown to occur due to a high ionization rate of the gases obtained by use of the FAES and their elevated energy when accelerated in the FAES [27].

TiN films deposited with and without employing the FAES were studied using scanning electron microscopy (SEM), high resolution scanning electron microscopy (HRSEM), atomic force microscopy (AFM) and optical microscopy. The X-ray studies of the films were performed using a DRON-2M X-ray diffractometer. Residual stresses were examined by use of the standard $\sin^2\Psi$. The crystal lattice parameters were determined by use of the (1 1 1) reflection. Harmonic analysis of the reflection shape using the (1 1 1) and (2 2 2) reflections was employed to obtain data on dispersion of microdistortion in the TiN crystal lattice.

The microhardness of the films was measured using a PMT-3 instrument at a load of 0.5 N.

The relative fracture toughness value of the TiN films was estimated by a conventional method including measurement of the total length of the Palmquist cracks after the Vickers indentation. The toughness of the coated steel substrate was estimated from the ratio between the load utilized for the indentation and the average length of the Palmquist cracks near the indentation. The value obtained in this way can be considered as a relative one, because it is affected by the film thickness, adhesion, hardness, etc., as well as some properties of the substrate. Nevertheless, this value appears to be helpful in estimating the performance of the deposited films when utilized in wear applications, because it characterizes fracture toughness of the near-surface layer of the coated specimen.

The adhesion of the films was measured using the conventional scratch test method when scratching the coated steel specimen with a Vickers tip at a load of 5 N. The adhesion value was determined by measuring the total film exfoliation square and the coefficient of adhesion was calculated as a ratio of the scratch square to the exfoliation square together with the scratch square. The method employed in the present study is thought to be more precise than the conventional scratch test method with the coating exfoliation being determined by acoustic emission means, because it is possible to eliminate errors related to failures in the coating volume appearing during scratching.

The performances of coated steel and cemented carbide tools were examined in turning and milling of carbon steel. The protective properties of the TiN films were also examined in field tests when employed as wear-resistant coatings for components of a piston pump.

3. Results and discussion

3.1. The influence of the FAES operational parameters on the deposition rate

The deposition rate using FAES is affected mainly by four parameters: an arc current, a current running in the induction coil, a bias voltage between the bodies of the PVD unit and the FAES, and the substrate biasing. In the present study the arc current was constant and equal to 100 A; the influence of the other three operational parameters on the deposition rate was investigated.

Fig. 2 shows curves indicating the influences of the substrate biasing and bias voltage applied to the body of the FAES on the deposition rate. The deposition rate rises with decreasing substrate biasing, which is typical for a conventional arc-evaporation PVD procedure, and with increasing bias voltage applied to the FAES body; which means that a higher amount of Ti ions is fed to the substrate surface.

Fig. 3 exhibits the influence of the induction coil current on the deposition rate at different values of the bias voltage applied to the body of the FAES. The deposition rate slightly rises with increasing current value because of the focusing of Ti ions in the centre of the deposition zone. The deposition rate significantly grows with increasing bias voltage from 10 to 20 V. One should note that, presumably, deposition does not occur when these two parameters are equal to zero, i.e. penetration of metal ions from the FAES into the

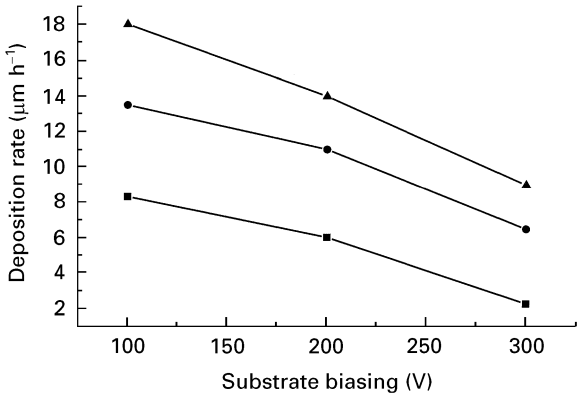

Figure 2 Deposition rate versus substrate biasing with (■) 10, (●) 15 and (▲) 20 V bias voltage applied to the body of the FAES.

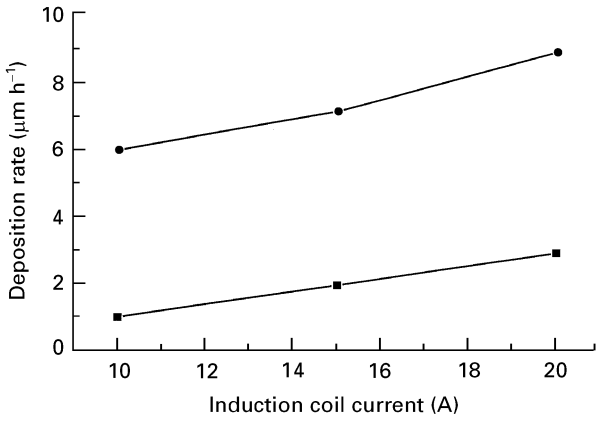

Figure 3 Deposition rate versus induction coil current at (■) 10 and (●) 20 V bias voltage applied to the body of the FAES.

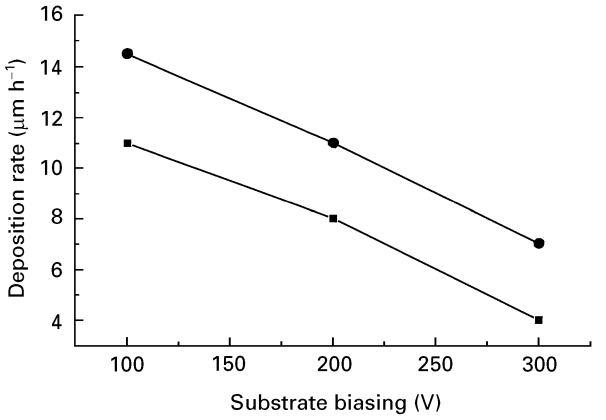

Figure 4 Deposition rate versus substrate biasing at (■) 10 and (●) 20 A induction coil current.

internal space of the PVD unit can be completely prevented by varying the induction coil current and bias voltage.

Fig. 4 shows the influence of the substrate biasing on the deposition rate at different values of the induction coil current. The deposition rate increases simultaneously with the decreasing biasing applied to the substrate and increasing current value.

Fig. 5 indicates the influence of the induction coil current on the distribution of the coating thickness within the deposition zone. The non-uniformity of the deposition rate in the deposition zone becomes more distinct when increasing the current value due to focusing the ion beam into the centre of the deposition zone. One can see in Fig. 5 that a relatively uniform coating is deposited within the deposition zone up to 20 cm in diameter at a current value of 6 A.

3.2. Structure of the TiN films

Fig. 6 shows the microstructure of the near-surface layer of WC–Co hard metal after its bombardment with Ti ions under parameters typically applied in conventional steered arc-evaporation deposition of TiN films. It is clearly seen that a noticeable decarburization of the substrate takes place in this case, leading to the formation of a decarburized η-phase (Co_3W_3C) underlayer in the near-surface layer of the hard metal

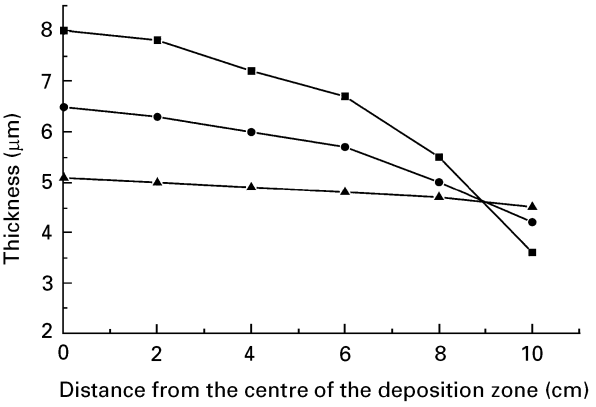

Figure 5 TiN film thickness versus distance from the centre of the deposition zone at (▲) 6, (●) 10 and (■) 20 A induction coil current.

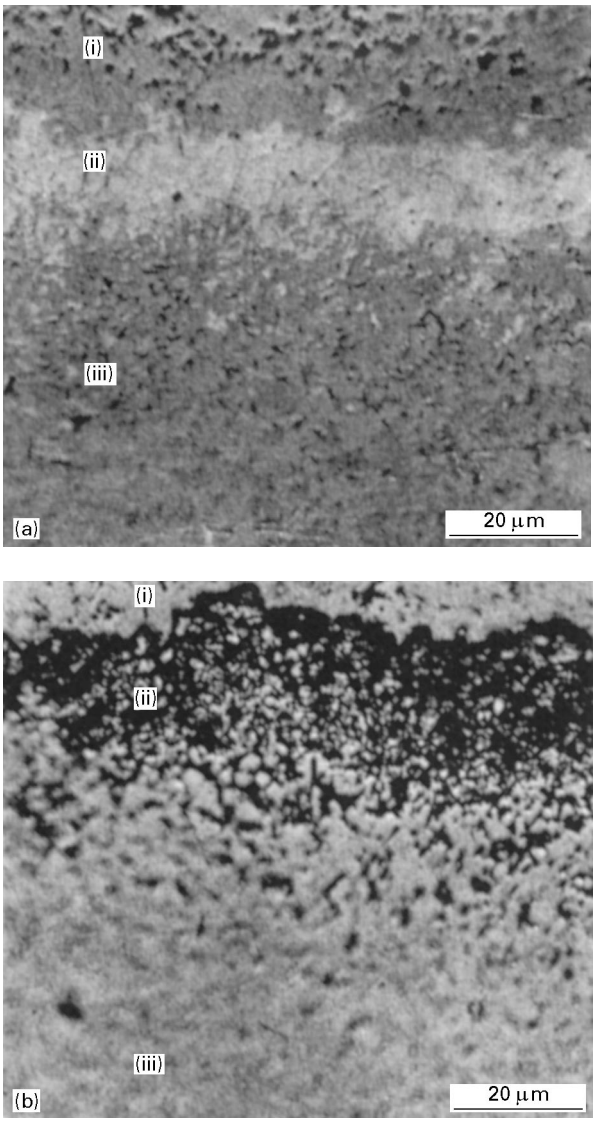

Figure 6 Microstructure of WC–Co hard metal bombarded with Ti ions by use of steered arc-evaporation. Tapered cross-sections: (a) before (η-phase not etched) and (b) after etching (η-phase etched) in the Murakhami reagent. (i) TiC film, (ii) η-phase, (iii) substrate.

substrate. Formation of this underlayer in the hard metal substrate has been shown to lead to a noticeable decrease in the coating adhesion resulting in its reduced performance [8].

Fig. 7a–c shows the morphology and microstructure of TiN films deposited onto the cemented carbide substrate using the conventional steered arc-evaporation procedure. It is clearly visible that the coating comprises macroparticles of the Ti-based droplet phase and has a relatively coarse, columnar structure.

Fig. 8 shows tapered cross-sections of the TiN films deposited using either steered arc-evaporation or filtered arc-evaporation after etching in a mixture of diluted HNO_3 and HF, which ensures dissolution of the Ti-based droplet phase. It is seen that the TiN film

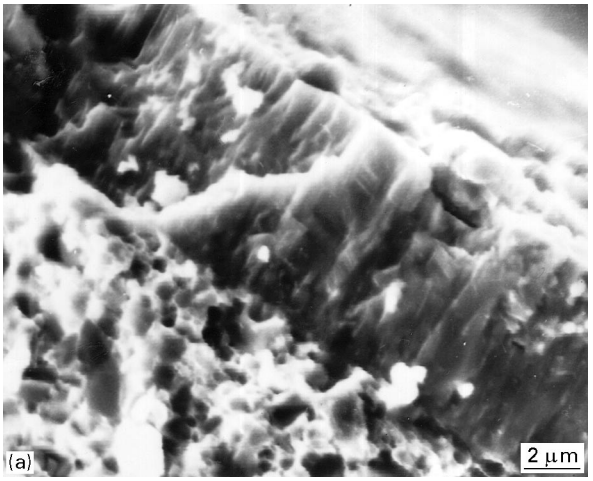

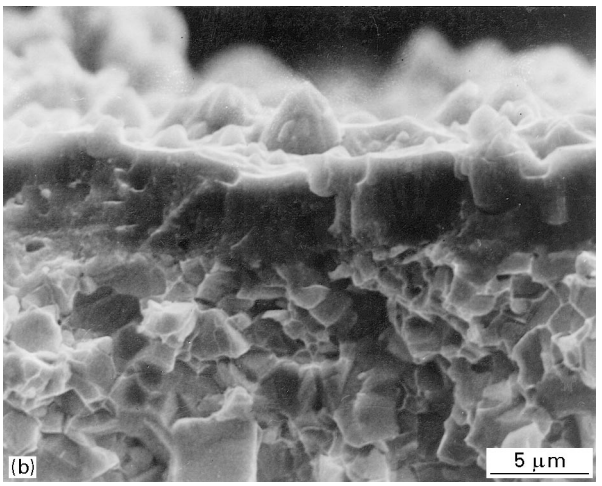

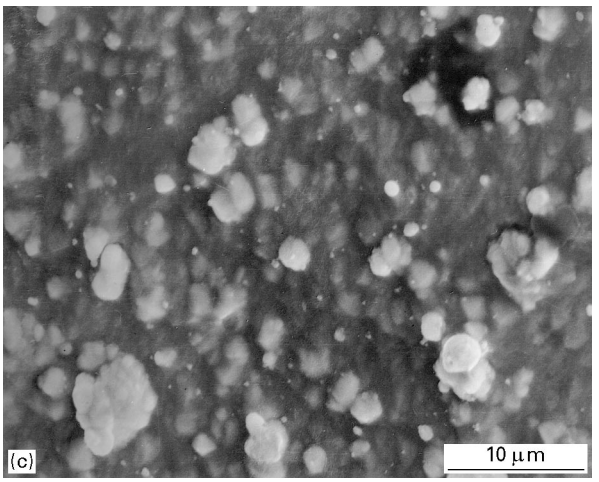

*Figure 7*a–c Microstructure and morphology of TiN coatings deposited by steered arc-evaporation.

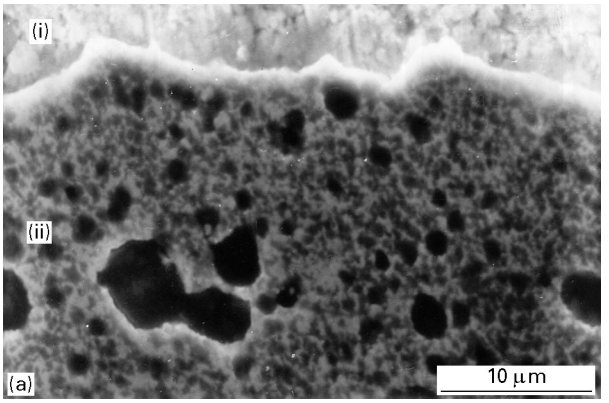

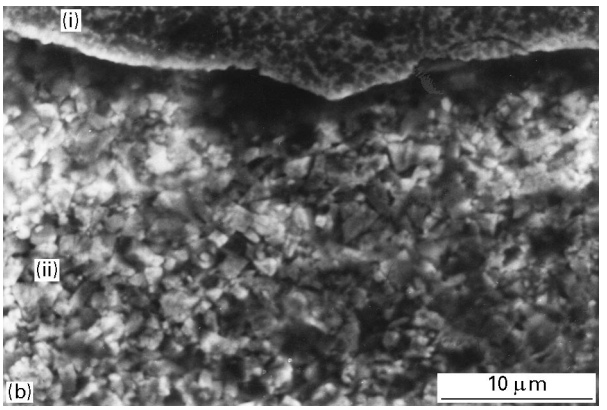

Figure 8 Microstructure of WC–Co hard metal with TiN coatings deposited by (a) steered and (b) filtered arc-evaporation. Tapered cross-sections after etching in a mixture of diluted HNO_3 and HF: (i) substrate, (ii) coating.

obtained by steered arc-evaporation comprises a great number of micro- and macroparticles of the Ti-based phase (which are etched away and look like dark holes). These Ti-based inclusions range from <1 to $\sim 10\,\mu m$ in size. Although steered arc-evaporation allows some decrease in the number of Ti-based macroparticles, Ti-based microparticles around 1 μm in size can hardly be eliminated in this way. The TiN film deposited using filtered arc-evaporation is highly uniform and absolutely free of micro- and macroinclusions of the Ti-based phase. Fig. 8b shows that the filtered arc-evaporation procedure preserves the hard metal substrate from decarburization and damage, because maintenance of the hard metal structure directly under the coating takes place. This can presumably be achieved due to heating the substrate up to the deposition temperature using only Ar ions instead of Ti ions typically employed in conventional arc-evaporation PVD procedures.

Fig. 9a–d shows the morphology and microstructure of the TiN film deposited using filtered arc-evaporation. It is seen that the surface of the film is macroparticle-free and smoother than the conventionally deposited TiN coating. The film has a finer structure compared with conventionally deposited TiN films; however, by the photomicrographs shown in Fig. 9, which were obtained using a low resolution SEM, it is impossible to investigate the fine coating structure.

The fine structure of the TiN film deposited by filtered arc-evaporation is clearly seen using HRSEM

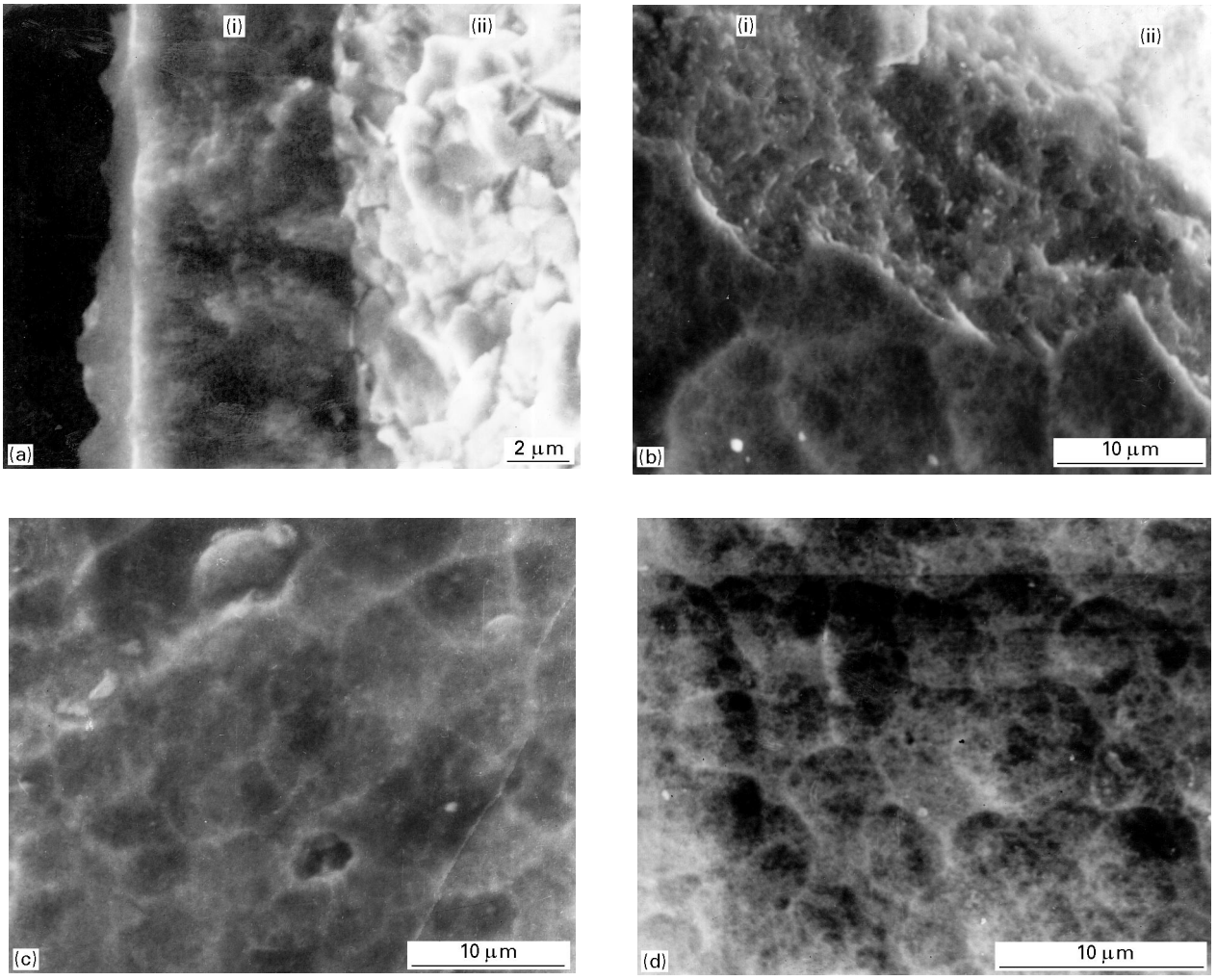

*Figure 9*a–d SEM microstructure and morphology of TiN films deposited onto WC–Co hard metal by filtered arc-evaporation: (i) coating, (ii) substrate.

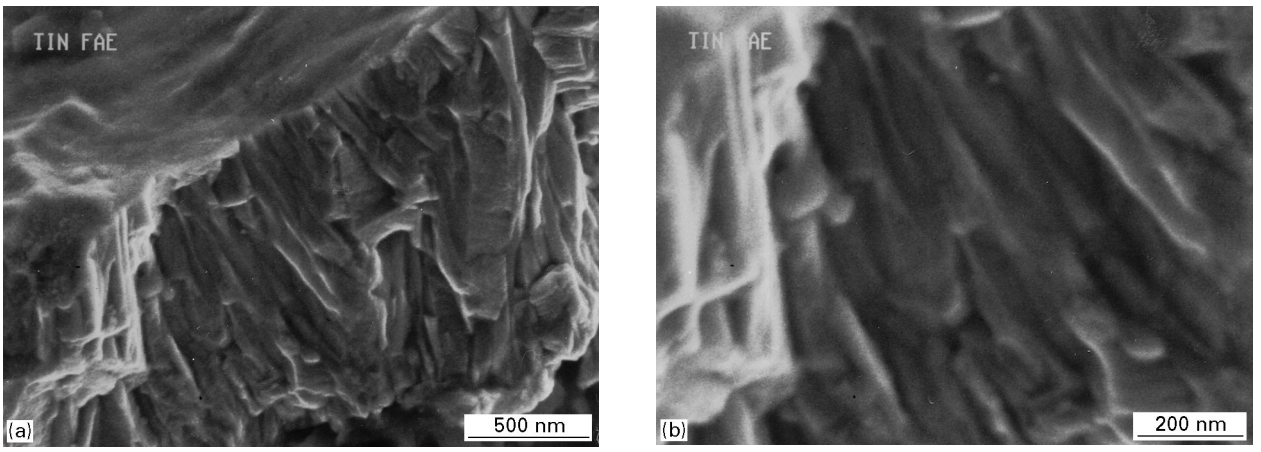

*Figure 10*a,b HRSEM microstructure of TiN films deposited by filtered arc-evaporation.

(Fig. 10). One can see that the film comprises columnar nanocrystals of <100 nm in diameter. The tips of these crystals at the surface of the film are shown in Fig. 11, which was obtained with the aid of AFM. Fig. 11 shows that the surface of the film is quite uniform and comprises structural units varying from a few nanometres to several tens of nanometres in size. It has been found that the microroughness of the film, i.e. the difference in height among the tips of the structural units and their boundaries, is within 100 A. The formation of the nanograined structure of the TiN films is presumably related to the noticeable difference in the nature of plasmochemical synthesis occurring during filtered arc-evaporation compared with conventional arc-evaporation techniques, mainly the higher ionization rate of both titanium and nitrogen [24, 27].

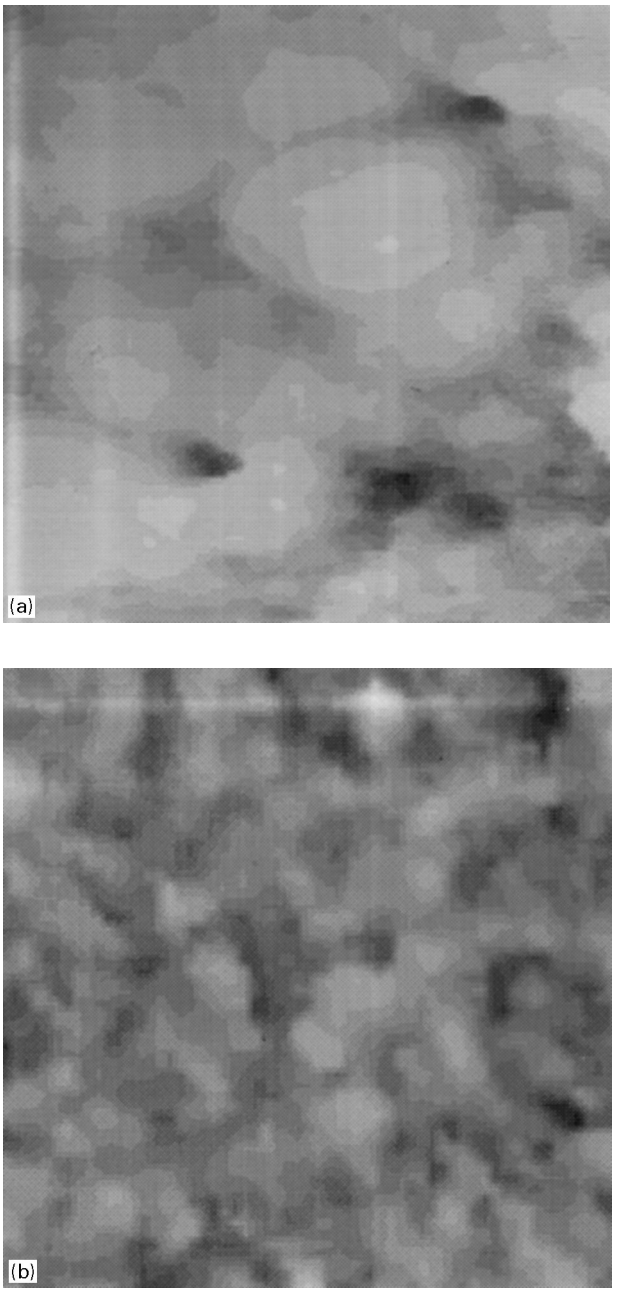

Figure 11 AFM surface structure of TiN films deposited by filtered arc-evaporation at (a) 250.5 A^2 and 2502.7 A^2.

3.3. Properties of TiN films deposited using filtered and steered arc-evaporation

3.3.1. Microdistortions, texture and parameters of the crystal lattice

Different nitrogen pressure values were utilized when applying conventional steered arc-evaporation to achieve approximately the same deposition rate in both the steered and filtered arc-evaporation procedures. This was related to the occurrence of different deposition rate values at the same nitrogen pressure value with and without the use of FAES. The properties of the TiN films were compared when either the nitrogen pressure or the deposition rate were equal to each other in steered and filtered arc-evaporation.

Table I shows some characteristics of the TiN crystal lattices of the films deposited in these ways. The employment of FAES leads to a slight increase in the crystal lattice parameter value of TiN deposited at the same nitrogen pressure value.

Table I also indicates that dispersion of microdistortion in the TiN crystal lattice, which characterizes the rate of microdeformation of the crystal lattice, is slightly lower when applying filtered arc-evaporation than when applying steered arc-evaporation, being employed at the same nitrogen pressure value. Meanwhile, the rate of microdistortion of the TiN crystal lattice obtained at the same deposition rate is approximately the same with and without employing FAES.

Table I indicates that all the TiN films investigated are characterized by the presence of (1 1 1) axial texture. TiN deposited by filtered arc-evaporation has a lower texture rate, which is obviously related to the growth of slightly less orientated, nanograined crystals in the case where FAES is employed. The TiN films deposited when employing FAES are found to be characterized by a different rate of formation of axial texture depending on the substrate biasing value. Whereas these films are characterized by only weak (1 1 1) texture when the substrate bias is absent, strong (1 1 1) texture and less distinct (1 1 0) texture appear upon increasing the biasing value up to 50 V. The texture of both types becomes more distinct upon increasing the substrate biasing current up to 200 V. This is obviously related to preferred sputtering-away of randomly orientated crystals when increasing the substrate biasing value.

Table I also shows the values of the residual stresses for the TiN films deposited by filtered and steered arc-evaporation. The films deposited with the aid of FAES are found to be characterized by higher level of residual stresses than those deposited conventionally, which is evidently determined by their nanograined structure.

3.3.2. Toughness, microhardness and adhesion

Fig. 12 shows the average length of the Palmquist cracks near the Vickers indentations as a function of the load utilized for the TiN films deposited onto the steel substrate using either steered or filtered arc-evaporation. It is seen that the films deposited using filtered arc-evaporation have an improved toughness compared with those deposited by steered arc-evaporation. This is evidently a result of their far finer structure and uniformity as well as the absence of the droplet phase in the structure. Better toughness of these films is assumed to result in their improved resistance to high static and impact loads when employed as wear-resistant coatings for tools and wear parts.

Fig. 13 shows the dependence of fracture toughness upon substrate biasing value for films deposited either by steered or filtered arc-evaporation. The fracture toughness of the films deposited with the aid of FAES is much higher than that of the films deposited conventionally, especially at relatively low substrate biasing values. Fracture toughness decreases with increasing substrate bias voltage. This is evidently related to some decrease in the adhesion of coatings and increase in their brittleness at high substrate biasing.

TABLE I Some characteristics of TiN films deposited with and without the use of FAES

Technique	Deposition rate ($\mu m\ h^{-1}$)	Nitrogen pressure (Pa)	Axial texture (1 1 1)	Crystal lattice parameter (nm)	Residual stresses (MPa)	Dispersion of microdistortion of crystal lattice ($\times 10^{-3}$)
Conventional	8	0.4	Strong	0.4249	−1300	3.9
Conventional	6	2.7	Strong	0.4237	−1700	2.0
With FAES	6	0.4	Medium	0.4254	−3300	2.6

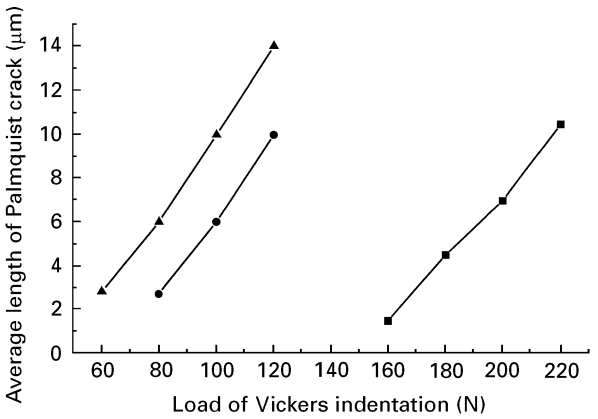

Figure 12 Average length of Palmquist cracks versus load of Vickers indentation of TiN films deposited by (●, ▲) steered, at 2.7 and 0.4 Pa, respectively, and (■) filtered, at 0.4 Pa, arc-evaporation.

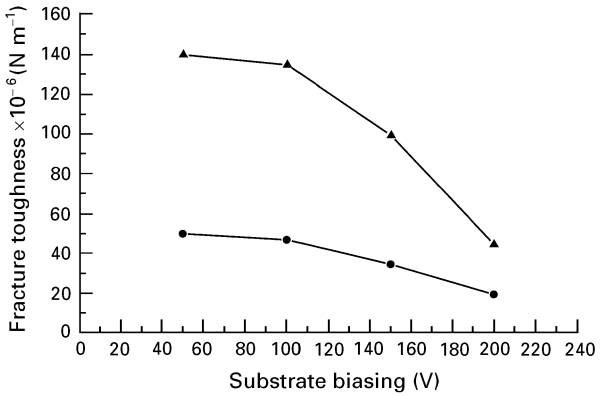

Figure 13 Fracture toughness versus substrate biasing of TiN films deposited by steered (●) and filtered (▲) arc-evaporation.

Fig. 14 shows the microhardness of the TiN films deposited with and without the aid of FAES as a function of substrate biasing. The microhardness of the films deposited by filtered arc-evaporation grows with increasing substrate biasing and reaches a level of about 37 GPa, which is much higher than that of TiN deposited using conventional steered arc-evaporation. Such a high microhardness value for the films deposited using FAES is evidently related to their nano-grained microstructure and the absence of a Ti-based droplet phase.

Adhesion of the coatings to the steel substrate has been determined to be affected significantly by the deposition technique employed. Whereas the coefficient of adhesion of the TiN films deposited using steered arc-evaporation typically ranges from 0.3 to 0.6 depending on the deposition parameters, that of the films deposited using filtered arc-evaporation ranges from 0.8 to 1.0. This noticeable difference in the adhesion level is evidently related to more effective substrate cleaning and heating-up due to the use of high-energy Ar ions instead of Ti ions and the absence of a droplet phase at the substrate–coating interface. It should be noted that whereas the TiN films deposited by steered arc-evaporation have very poor adhesion without applying the substrate biasing, those deposited using FAES have an acceptable level of adhesion even when the substrate biasing value is equal to zero. This is presumably related to the higher energy of ions achieved by their acceleration under the influence of magnetic and electric fields in the volume of the FAES. Obviously, such ions can reach the substrate surface with energies suitable to achieve an acceptable level of adhesion without applying any substrate biasing.

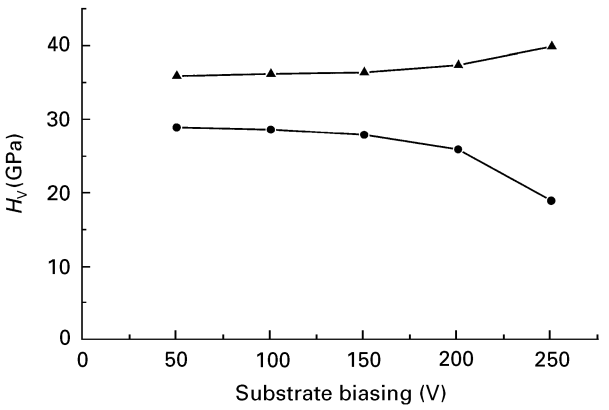

Figure 14 Vickers hardness versus substrate biasing of TiN films deposited by steered (●) and filtered (▲) arc-evaporation.

3.3.3. Performance properties

Fig. 15 shows the relative tool lifetime values of the coated hard metal and HSS tools in turning and milling. It is seen that around a two-fold increase in tool lifetime is achieved when employing TiN coatings deposited by filtered arc-evaporation instead of those deposited conventionally. This is presumably a result of the enhanced adhesion, fracture toughness and hardness of the TiN films obtained when employing filtered arc-evaporation. The improved fracture

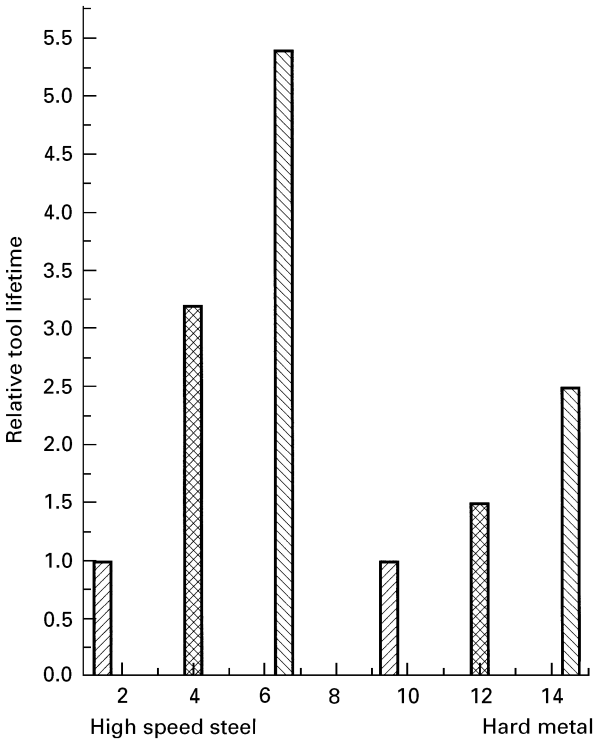

Figure 15 Lifetime of cutting tools with TiN coatings deposited by steered (▨) and filtered (▨) arc-evaporation until a flank wear of 0.8 mm is obtained for HSS tools and 0.5 mm for hard metal tools. The cutting conditions for HSS tools: turning carbon steel; cutting speed, 100 m min^{-1}; feed, 0.3 mm rev^{-1}; depth, 0.5 mm; and flank wear, 0.8 mm. Cutting conditions for hard metal tools: milling carbon steel; cutting speed, 200 m min^{-1}; feed, 0.2 mm rev^{-1}; depth, 1.0 mm; and flank wear, 0.5 mm. (▨) substrate.

toughness of the TiN films is especially important in interrupted cutting, e.g. in milling, when the coating is affected by high impact loads. The better performance of the films deposited by filtered arc-evaporation is presumably also related to their improved surface roughness and the absence of droplet Ti-based phase, which can reduce the interaction rate between the coating and workpiece material in metal-cutting.

The TiN films deposited by filtered arc-evaporation were also examined in field tests as wear-resistant coatings for precise surfaces of plungers for piston pumps. The plunger surface of the pump must have an excellent surface finish, which cannot be achieved using conventional arc-evaporated PVD coatings because of the presence of a droplet phase at their surfaces. The TiN films deposited by filtered arc-evaporation were determined to have excellent surface roughness, which allowed their successful employment as wear-resistant coatings for piston pump plungers. As one can see in Fig. 16, the service lifetime of the plungers after coating was up to six times higher than that of the uncoated plungers and the stability of the rated cyclic feed of the coated plungers unit was enhanced 7.5 times with the aid of TiN coatings deposited by filtered arc-evaporation.

4. Conclusions

The employment of filtered arc-evaporation allows nanograined, smooth, uniform and droplet-phase-free

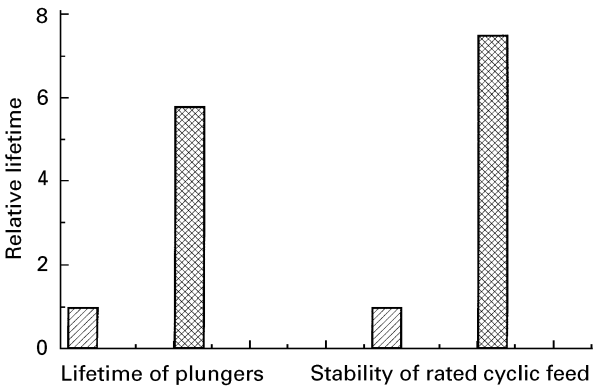

Figure 16 Performance of piston pump plungers with TiN coatings deposited by filtered arc-evaporation. (▨) substrate, (▨) TiN coated plunger.

TiN coatings to be deposited onto steel and hard metal substrates without any damage to the substrate or decarburization. These coatings are characterized by a slightly higher crystal lattice parameter, lower rate of axial (1 1 1) texture and higher residual stresses compared with TiN coatings deposited by conventional steered arc-evaporation. The coatings deposited by filtered arc-evaporation have an improved fracture toughness, hardness and adhesion, which results in their better performance in sliding and cutting applications.

Acknowledgements

The authors would like to thank Professor G. Petzow for helpful discussion and Professor V. Panov for AFM studies of TiN films.

References

1. A. MATTHEWS and A. R. LEFKOW, *Thin Solid Films* **126** (1985) 283.
2. J. E. DAALDER, *J. Phys. D* **9** (1976) 2379.
3. *Idem*, *Physica C* **104** (1981) 91.
4. H.-D. STEFFENS, M. MACK, K. MOEHWALD and K. REICHEL, *Surf. Coating Technol.* **46** (1991) 65.
5. H. RHANDHAWA and P. C. JOHNSON, *ibid.* **31** (1987) 303.
6. E. ERTUERK, H.-J. HEUVEL and H.-G. DEDERICHS, *ibid.* **39/40** (1989) 455.
7. V. M. LUNEV, V. D. OVCHARENKO and V. M. KHOROSHIKH, *Sov. Phys-Tech. Phys.* **22** (1977) 855.
8. I. KONYASHIN, E. LEONOV, A. ANIKEEV and A. ZARAHKANI, *Sov. Powder Met. Metals Ceramics* **28** (1990) 816.
9. I. KONYASHIN, A. ZARAHKANI and E. LEONOV, *Sov. J. Non-Ferrous Met.* **5** (1988) 76.
10. I. KONYASHIN, *Surf. Coating Technol.* **71** (1995) 277.
11. A. ERDEMIR and C. CHENG, *J. Vac. Sci. Technol. A* **7** (1989) 2486.
12. J.-E. SUNDREN, *Thin Solid Films* **128** (1985) 21.
13. I. AKSENOV, V. BELOUS, V. PADALAKA and V. KHROSHIKH, *Sov. J. Plasma Phys.* **4** (1979) 425.
14. A. DORODNOV, S. MUBOYDZHAN, Y. PAMELOV and A. STRUKOV, *J. Appl. Mech. Tech. Phys* **22** (1981) 28.
15. I. DEMIDENKO, N. LOMINO and V. PADALKA, *Sov. Phys. Tech. Phys* **21** (1976) 284.
16. D. SANDERS and E. PYLE, *J. Vac. Sci. Technol. A* **5** (1987) 2728.
17. D. SANDERS, *ibid.* **7** (1989) 2339.

18. V. CHERNYAEV and V. KARZE, *Radio Electron. Commun. Syst*. **25** (1982) 68.
19. I. AKSENOV, V. BELOUS, V. PADALKA and V. KHOROSHIKH, *Instrum. Exp. Tech.* (*USSR*) **21** (1978) 2.
20. I. AKSENOV, A. BELOKHVOSTIKOV, V. PADALKA, N. REPALOV and V. KHOROSHIKH, *Plasma. Phys. Contr. Fussion* **28** (1986) 761.
21. A. DORODNOV and S. MIROSHKIN, *High Temp.* (*USSR*) **18** (1980) 821.
22. I. AKSENOV, V. BREN, V. PADALKA and V. KHOROSHIKH, *Sov. Phys. Tech. Phys.* **7** (1981) 497.
22. K. AKARI, H. TAMAGAKI, T. KUMAKIRI, K. TSUJI, E. KON and C. TAI, *Surf. Coating Technol.* **43/44** (1990) 312.
23. C. TAI, E. KON and K. AKARI, *Surf. Coating Technol.* **43/44** (1990) 324.
24. P. MARTIN, R. NETTERFIELD, A. BENDAVID and T. KINDER, in Annual Technical Conference Proceedings of the Society for Vacuum Coaters (Society of Vacuum Coates, Boston, 1993) p. 375.
25. P. MARTIN, R. NETTERFIELD and T. KINDER, *Int. Appl.* **16** (1992) 959.
26. P. MARTIN, R. NETTERFIELD, A. BENDAVID and T. KINDER, *Surf. Coating Technol.* **136** (1992) 54.
27. G. BARINOV, A. DODONOV and V. OGAY, "Ion-plating technology", (Machinostroenie, Moscow, 1987) p. 34.
28. I. AKSENOV, Y. ANTUFEV and V. BREN, *Phys. Chem. Mater. Treatment* **4** (1981) 43.

Received 19 April 1996
and accepted 2 April 1997